Textures and Microstructures, Vol. 29, pp. 155–183
Reprints available directly from the publisher
Photocopying permitted by license only

CALCULATION OF TEXTURE VOLUME FRACTIONS BY INTEGRATION AND GAUSSIAN FITTING

M.B. CORTIE

Mintek, Private Bag X3015, Randburg 2125, South Africa

(Received 25 August 1996)

The concept of texture volume fractions has proved useful in the assessment of the orientation distributions of polycrystalline samples. Unfortunately, there is more than one method of calculating volume fractions, and the different techniques may give rather different answers. The three most commonly used methods appear to be calculation from the coefficients of the harmonic function, integration over a selected portion of an orientation distribution function (ODF), or decomposition of an ODF into component Gaussian ideal textures by a least squares fitting. The integration and Gaussian fitting methods are examined further here. In particular, the nature of the errors or differences arising from the method of integration or fitting chosen, the differing interpretations of the shape and 'spread' of the ideal texture, and the effect of neglecting texture components lying outside of the H^0 subspace are considered. Integration of a volume enclosed by one or more cylinders defined in Eulerian space seems the most robust technique. It is usually, but not always, acceptable to neglect the effect of texture components lying outside of H^0. However, it is vital that the 'spread' of the ideal texture component be precisely defined, and the texture volume fraction is very sensitive to the magnitude of the spread as well as to the geometric shape assumed for it.

Keywords: Volume fractions; Ideal orientation; Gaussian spread; Comparison of methods

INTRODUCTION

Orientation distribution functions (ODFs) are widely used to describe the crystallographic texture of polycrystalline materials. The trained eye can, with some assistance from tables of ideal orientations, readily identify the predominant textures in a graphical rendition of an ODF. However, while this qualitative type of examination serves in many

situations, a more quantitative approach is often more appropriate for systematic work. The most basic requirement of the quantitative approach is a measure of the 'strength' of a given sample's texture, relative to that of a random or other sample. The texture index, J, is often used in this role, although the maximum intensity value on an ODF is also useful. Another technique is to plot cross-sections of ODF value versus Euler co-ordinate, and in this way examine some relevant slice through orientation space. This method may be used to determine, with reasonable security, whether a particular orientation or fibre is more strongly developed in a certain specimen than another. Less frequent use is made of the concept of texture volume fractions as a method of comparing textures, although they have been widely harnessed in algorithms for the elimination of the so-called 'ghost peaks' in an ODF (Lücke *et al.*, 1986). Some authorities have stated that texture volume fractions are of little use in a metallurgical sense because the concept is poorly defined, has little physical significance and the quantities are difficult to reproduce between laboratories. It will be shown here, however, that texture volume fractions not only possess a physical reality, but that they can be unambiguously, reproducibly and simply determined.

The work described was initially prompted by the need to explain discrepancies in the texture volume fractions calculated at Mintek compared to those obtained by an established industrial laboratory. The samples in question were of aluminium alloy 3004, pieces of which had been subjected to various thermo-mechanical treatments. The calculation of texture volume fractions has enjoyed some use in the aluminium industry – see for example, Jensen *et al.* (1994). This may be because control of the texture is very important in the manufacture of aluminium beverage-can body and end-cap material.

Two numerical methods by which texture volume fractions can be readily and reproducibly determined are assessed. These are termed here the integration method and the Gaussian fitting method. An alternative method in which the volume fraction is calculated from certain coefficients generated during the spherical harmonic method of calculating an ODF, is not considered in any detail. An executable version of the computer program developed for this work is available for inspection. The discussion that follows applies exclusively to cubic materials and for orthorhombic sample symmetry.

PHYSICAL SIGNIFICANCE OF A TEXTURE VOLUME FRACTION

A polycrystalline sample of geometric volume V consists of an assemblage of individual grains i, each with its individual orientation and each of geometric volume v_i, such that $\sum v_i = V$. The volume fraction occupied by a particular grain, v_i, is a measurable physical quantity. In an assemblage consisting of a finite number of grains, very few grains will, in general, have orientations that *exactly* match any particular ideal orientation. In general there will be small deviations in orientation, either because of measurement errors or because of genuine physical variation. However, it may be useful to collect together all those grains with a *similar orientation* to that of the particular ideal orientation, and to sum the volume of those grains. It is assumed that the normalized intensity of the X-ray diffraction signal for a given orientation is proportional to the volume of material with that orientation. A texture volume fraction can then be calculated directly from an ODF, and is defined as the physical volume fraction of those grains that have an orientation in Euler space which is similar to that of an ideal component.

There are two steps in the determination of the volume fraction. In the first, a workable definition of the term *similar orientation* must be obtained. Following this, a method by which the necessary information can be extracted from, for example, an experimental ODF, must be developed.

Various ways of defining a similarity in orientation have recently been discussed by Bunge (1996), who examined, *inter alia*, the differences between texture components defined according to criteria such as 'vicinity' and those defined according to a mathematical function, very often a Gaussian. Both approaches have been examined in the present work.

The angular distance from a given position in Euler space is in general given by the minimum angular rotation, ω, required to bring the crystal axes of a given orientation into coincidence with that of the ideal orientation (Bunge, 1982; Hansen *et al.*, 1978). The orientation distance is

$$\omega = |g'(\varphi_1', \phi', \varphi_2') \cdot g(\varphi_1, \phi, \varphi_2)^{-1}|, \tag{1}$$

where g' is the rotation matrix of the ideal orientation in Euler space and g the rotation matrix of any other point in Euler space. The inverse of matrix g may be found by the usual techniques of linear algebra, or may be obtained (Bunge, 1982) by substituting $(\pi - \varphi_2)$ for φ_1, and $(\pi - \varphi_1)$ for φ_2 into $g(\varphi_1, \phi, \varphi_2)$. The operation $|\ |$ does not yield the determinant, but rather the 'absolute angular magnitude':

$$|g| = \arccos\{\tfrac{1}{2}(g_{11} + g_{22} + g_{33} - 1)\}, \tag{2}$$

where g_{ij} are the elements of the matrix g (Hansen *et al.*, 1978).
In the so-called 'vicinity' approach (Bunge, 1996) grains, and therefore by extension points on the ODF, with orientation distances less than ε angular units of the ideal orientation are considered to be part of that texture component, and those that have a greater angular deviation are not. The cut-off value, ε, could also be called the 'spread' of the texture component.

This 'vicinity' definition is not completely compatible with the common 'mathematical' definition of an ideal texture component as a Gaussian function (Bunge, 1982):

$$S(\omega) = S_0\, \mathrm{e}^{-\omega^2/\omega_0^2}, \tag{3}$$

where S_0 is the value of the function at $\omega = 0$, and ω_0 is the angular distance from the central point, or spread, at which the ODF value falls to 1/e of S_0 (Bunge, 1982; 1996). A particular difference compared to a vicinity definition is that, in this method, the width of the Gaussian function is *characterized*, but not *limited*, by its 'spread' parameter, ω_0. The tails of the Gaussian extend beyond this spread (Fig. 1), and their inclusion or exclusion can have a significant effect on the outcome of an analytical integration calculation (Bunge, 1996; Lücke *et al.*, 1986).

It follows therefore that, for a given 'spread', the volume fraction computed by integration could be much smaller than one computed analytically by assuming a Gaussian ideal texture component. Besides the complication of the 'tails', it will also follow that a scheme in which a Gaussian is *fitted* to data in an ODF will in general result in a variable best-fitting spread parameter, and will therefore give different results to some other scheme in which a fixed value of the spread parameter is assumed.

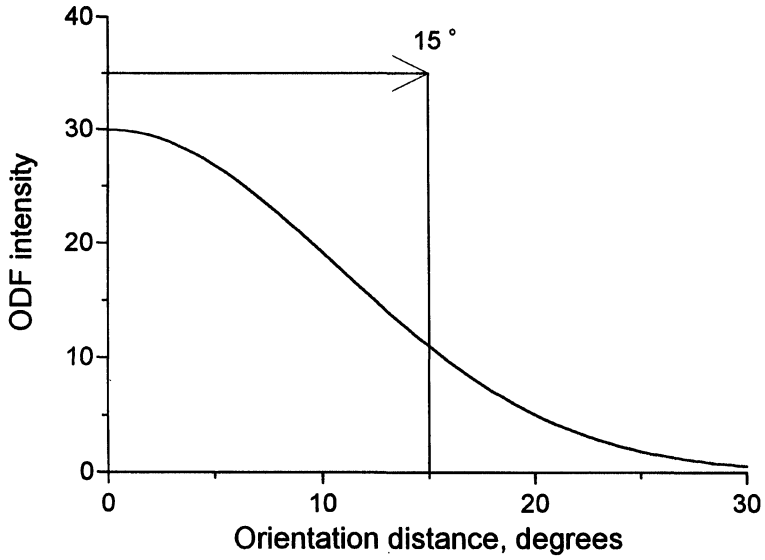

FIGURE 1 Comparison of the 'vicinity' and 'mathematical' definitions of similarity in texture and their effect on volume fractions.

In the particular instance where the ODF had been computed by the method of harmonic functions, the volume fraction occupied by a Gaussian texture component can also be directly calculated from the so-called 'C-coefficients' of the series expansion. This will be discussed later.

EXPERIMENTAL METHOD

Measurement of ODFs

Four industrial samples and a series of laboratory plane strain compression samples, all of aluminium alloy 3004, were used. All the samples were in the batch-annealed state except for industrial samples DDH and H19, which were in the as-rolled condition. The samples were polished to near the mid-plane and then electropolished in a solution of perchloric acid and ethanol. The samples were then analysed using a Siemens D500 X-ray diffractometer equipped with a Mo X-ray tube. The ODF maps were calculated using the 'popLA' program.

The same samples were then sent to the industrial laboratory, which was located in Europe, and were similarly analysed.

Calculation of Texture Volume Fractions

General

In general, the known methods of determining a texture volume fraction could be divided into the 'mathematical' group, which harness some aspect of the actual mathematical functions possibly used to generate and represent the ODF, and the 'numerical integration' group, in which the ODF is treated as a data structure that can be processed to yield selected information. In one of the most commonly used of the 'mathematical' techniques, the volume fraction of a Gaussian or fibre texture component is calculated from the C-coefficients of the series used to represent the ODF (for example Bunge, 1982; Zuo *et al.*, 1994). This method is, however, available only if the harmonic analysis method had been used to calculate an ODF from pole figure data, whereas the numerical integration and Gaussian fitting methods are, in principle, independent of the method used to measure, generate or calculate the ODF. These latter methods could be used even if the ODF were, for example, experimentally determined by exhaustive application of selected area diffraction. However, if the fall-off in intensities around the ideal component was not Gaussian, then use of the Gaussian-fitting method or indeed, the harmonic analysis technique, could be somewhat problematic in any case.

In one of the Gaussian fitting procedures – for example, Lücke *et al.* (1986) – the ODF is assumed to be the sum of several ideal orientations, each with a Gaussian spread from the respective Euler positions. The entire experimental ODF is decomposed into the component ODFs by a process of least squares minimization, and

$$f(g) \approx \sum_i V_i f_i^{\text{ideal}}(g), \tag{4}$$

where V_i is the volume fraction of ideal texture component $f_i^{\text{ideal}}(g)$, and $\sum V_i = 1$. This technique is sometimes used in the course of the calculation of an ODF from pole figure data as part of the algorithm

to eliminate ghosts (negative values) from the ODF. However, the algorithms used to decompose an ODF according to Eq. (4) have as their objective the minimization of the least-square deviation of the synthetic ODF compared to the starting ODF. Therefore their use to estimate the strength of individual texture components may be misleading. In the present work we will rather consider a modification of the single-point Gaussian fitting method mentioned in Bunge's (1982) textbook on texture.

As an alternative to the 'mathematical' methods, it is also possible to calculate the texture volume fraction by summing the ODF values that lie in the vicinity of the various ideal texture components. This approach will be termed here the 'volumetric integration' of an ODF file, and will be described in detail later.

The part of Euler space in which $0 < \varphi_2, \phi, \varphi_1 < \pi/2$ will be denoted here as the reduced subspace H^0 of the full Euler space H ($0 \leq \varphi_2, \phi, \varphi_1 \leq 2\pi$) in common with the notation outlined by Hansen *et al.* (1978). Of course, even this space contains redundancies, and in particular has three symmetrically equivalent subspaces of its own. Since the materials studied possessed a cubic crystal structure and the sample symmetry was orthorhombic, a consideration of H^0 would usually be sufficient. However, it will also be shown that consideration of positions lying outside of H^0 may be necessary in some cases.

Gaussian Spread Function

Bunge (1982) has described an approach in which the intensity at one of the crystallographically equivalent positions for the particular texture component is measured and converted to a texture volume fraction. The method requires that the texture component of interest is approximately Gaussian; however, this may often not be the case. The volume fraction is given by the expression (Bunge, 1982)

$$V_f = \frac{1}{\sqrt{4\pi}} Z \cdot S_0 \cdot \omega_0 \left[1 - e^{-\omega_0^2/4}\right], \tag{5}$$

where Z is the multiplicity factor of the particular texture component (being either 24, 48 or 96 depending on symmetry considerations), and S_0 and ω_0 are as previously defined. The latter two parameters must be

determined, either by inspection or by non-linear least-squares curve-fitting. With regard to the fitting, it may be worth pointing out that an attempt to determine the parameters by linearizing Eq. (3) by the taking of the logarithm of both sides will produce very inaccurate estimates of ω_0 and S_0. Accordingly, a non-linear least-squares regression technique was used in the present work. Data for the regression were obtained by scanning the ODF file and making a list of orientation distances to the nearest site of the particular ideal texture component, as calculated from Eqs. (1) and (2). Positions in the ODF lying at greater than 20° from an ideal site were discarded, since at that distance the individual positions are more likely to be part of some other texture component. An estimate of the goodness-of-fit was obtained by dividing the root mean square (RMS) error by the peak amplitude of the resulting Gaussian, to produce a 'relative RMS error'. Volume fractions associated with values of the relative RMS error greater than 25% were considered to be problematic.

Calculation of Volume Fraction by Integration in Euler Space

Since for any ODF

$$\frac{1}{8\pi^2}\int_0^{2\pi}\int_0^{\pi}\int_0^{2\pi} f(g)\cdot\sin\phi\cdot\mathrm{d}\varphi_1\cdot\mathrm{d}\phi\cdot\mathrm{d}\varphi_2 = 1, \tag{6}$$

a volume fraction can also be calculated by volumetric integration of some selected enclosed sub-volume of Euler space

$$V_\mathrm{f} = \frac{1}{8\pi^2}\int_{\text{vicinity}} f(g)\cdot\mathrm{d}g \tag{7}$$

where $\mathrm{d}g = \sin\phi\cdot\mathrm{d}\varphi_1\,\mathrm{d}\phi\,\mathrm{d}\varphi_2$. For example, the integral might be computed only over those regions of Euler space whose *orientation distance*, ω, from the ideal texture component of interest is less than ε angular units. Although the value of ε could be a constant, thereby giving a spherical volume in Euler space, it can also serve as the radius vector of a function defined on a set of cylindrical or spherical co-ordinates with their origin located on the position of the ideal orientation (Fig. 2). This is a more general method, since the actual shape of that portion of Euler space considered to lie within the

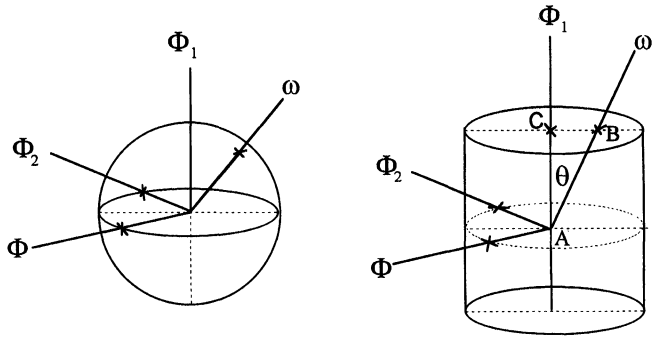

FIGURE 2 Spherical and cylindrical enclosures for use in volume fraction calculations.

vicinity of a given texture component can now be arbitrary. In addition, a given ideal orientation will in general occur more than once within the H^0 subset of Euler space (since there is threefold redundancy in that part of Euler space in which $0 < \varphi_2, \phi, \varphi_1 < \pi/2$) and the enclosing volumes may therefore become quite complex in shape. Furthermore, it is no longer necessary for the ODF to be computed using the series expansion method, and it could have been determined by any existing or future experimental or computational technique. Now even the volume fraction of complex components such as beta fibre of aluminium can be readily computed without requiring any extension to the method, provided only that the relevant enclosure within H^0 can be defined. There is no ambiguity in the above definition, since the ideal texture components can be precisely expressed as three-dimensional mathematical functions in Euler co-ordinates, as Boolean numerical arrays, as circle sweep solids, or in any other form that can define an enclosed volume of space.

The ODF map is then treated as experimental data of arbitrary internal structure and the volume fraction determined by volumetric numerical integration. Since the 5° step size usually used to store ODF files is a little coarse for these purposes, the ODF intensities were interpolated to a 2.5° step size and integration performed with a cube-shaped element. The volume fraction can then either be determined at one site and then multiplied by the factor arising from crystallographic symmetry, or by integration over all the symmetrically equivalent sites.

The angular distance, ω, can be calculated using Eqs. (1) and (2), or more conveniently, with the expression given by Lücke *et al.* (1986),

$$\omega = 2 \cdot \arccos\left[\cos\left(\frac{(\varphi_1' - \varphi_1) + (\varphi_2' - \varphi_2)}{2}\right)\cos\left(\frac{\phi'}{2}\right)\cos\left(\frac{\phi}{2}\right) + \cos\left(\frac{(\varphi_1' - \varphi_1) - (\varphi_2' - \varphi_2)}{2}\right)\sin\left(\frac{\phi'}{2}\right)\sin\left(\frac{\phi}{2}\right)\right], \quad (8)$$

where $(\varphi_1', \phi', \varphi_2')$ refers to the Euler co-ordinates of the nearest of the several equivalent ideal orientations. Eq. (8) gives the same result as the combination of Eqs. (1) and (2) in H^0, the subset of Euler space in which $0 < \varphi_1, \phi, \varphi_2 < \pi/2$. However, there are significant differences outside of H^0.

While the spherical ideal texture component (Fig. 2) was obviously obtained for

$$\omega \leq \varepsilon = \text{constant}, \quad (9)$$

a cylindrical element has, in this approach, to be computed by calculating the dot product between vectors AB and AC in Fig. 2, and then, depending on the value of angle θ, evaluating whether location ω lies inside or outside of the enclosed volume. Cylindrical elements seem to be quite frequently used (e.g. Flowers, 1983).

The partial integration of an ODF using Eq. (7) has been termed *Eulerian integration* here and, similarly, the orientation distances defined by Eqs. (1), (2) and (8) termed the *Eulerian distances*. It should be noted that there are other integration schemes too. For example, Ito *et al.* (1983) obtained volume fractions by integrating selected regions of suitable pole figures.

An Over-simplification: the Calculation of Volume Fraction in Euclidean Space

A simple approach to determining texture volume fractions might involve simply summing the ODF values that lie within a spherical region of specified radius around one of the manifestations of the desired texture in H^0, multiplying this answer by the multiplicity factor associated with that orientation, and dividing by the sum of all the values in the ODF.

The method may be expressed as

$$V_f \approx M \cdot \frac{\sum_{\varphi_2,\phi,\varphi_1}^{\text{ideal}} f(g)}{\sum_{\varphi_2,\phi,\varphi_1}^{\text{odf}} f(g)}, \tag{10}$$

where M is a symmetry multiplicity factor related to the number of times that the given ideal texture component occurs in a complete unit of Euler space, and the orientation distance is calculated by treating Euler space as Euclidean in co-ordinates $\varphi_2, \phi, \varphi_1$.

It is important to note that many simplifying assumptions have been made. For a start, as a method of volumetric integration, it is correct only in the limit of an infinitesimally small ODF step size. Secondly, by analogy with the properties of Euclidean space, the distance between two points $g(\varphi_2, \phi, \varphi_1)$ and $g(\varphi_2', \phi', \varphi_1')$ is given by

$$\Delta g \approx \sqrt[2]{(\varphi_2 - \varphi_2')^2 + (\phi - \phi')^2 + (\varphi_1 - \varphi_1')^2}. \tag{11}$$

However, it is important to note that Eq. (11) provides somewhat different values of orientation distance than Eqs. (1) and (2). Naturally, a cylindrical or other volume to be integrated can also be defined in this method. I will term this method the single-point-simplified Euclidean (SPSE) method in the discussion to follow.

Ideal Texture Components

Two synthetic ODFs were also used in the assessment: a random one in which $f(g)$ was everywhere equal to 1.0 (denoted as 'random' in the tables to follow) and an ODF comprised only of a cube texture with a 15° spread ('cube'). Each was normalized so that the volumetric integral (Eq. (6)) over the entire ODF equaled 1.0. The ideal textures were automatically computed by an algorithm that generated all the valid permutations of the relevant {hkl}[uvw], and which then calculated the corresponding values of φ_2, ϕ and φ_1. All components inside H^0 and those lying within 25° of one of the H^0 boundaries were considered. Ambiguities in the trigonometric equations when applied outside of H^0 were resolved by algebraic manipulation.

The ideal distributions calculated by the author's software were essentially identical to those previously reported for the various ideal textures. The spatial distortion in Euler space is clearly evident in the ϕ sections of, for example, the ideal copper texture, $\{121\}[1\bar{1}1]$, shown in Fig. 3. It is clear that the volumes around the equivalent ideal orientations have been dilated in the $\varphi_1+\varphi_2 = constant$ direction. However, it can be seen that the extent of this dilation diminishes as ϕ approaches 90°.

The software used by the industrial laboratory did not require the calculation of a full ideal texture component, and instead required the

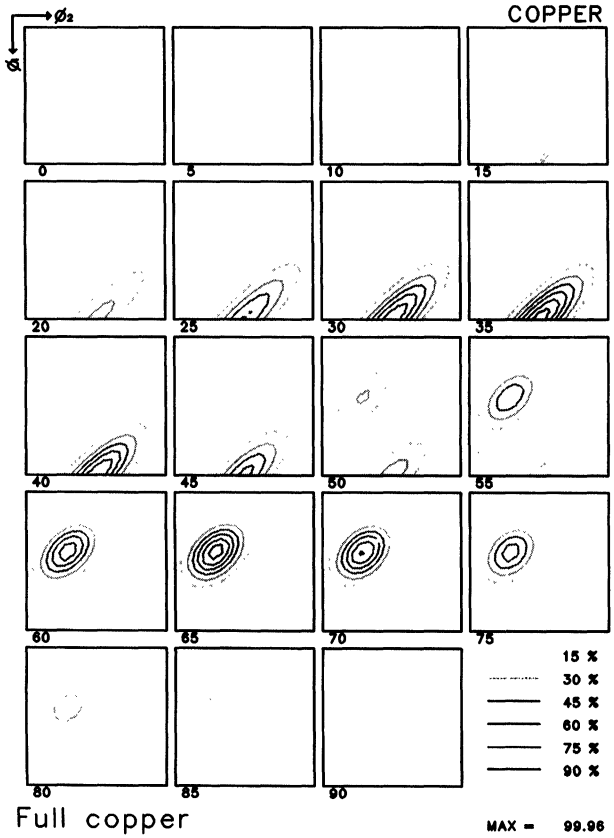

FIGURE 3 ϕ sections of an ideal copper texture calculated with a spread of 15° showing characteristic distortion in $\varphi_1 + \varphi_2 = constant$ direction.

TABLE I Summary of Euler angles used for single site estimations of volume fractions

Component	*Industrial laboratory*			*Alternative set*		
	φ_1	ϕ	φ_2	φ_1	ϕ	φ_2
Cube	90	90	90	0	0	0
Goss	90	90	45	0	45	0
Brass	55	90	45	35	45	0
Copper	39	66	27	90	29	45
S	53	74	34	59	29	63

input of one of the symmetrically equivalent positions of the component. Two spread parameters, each of 15°, were used, indicating the software invoked a cylindrical enclosure. Although the program evidently worked by integration over a region of the ODF, the detailed nature of the algorithm it used was not known. The positions used by the industrial laboratory for calculating the volume fractions are listed in Table I, together with an alternative and equivalent set used at Mintek when trying the SPSE method.

Influence of the Enclosure-Generation Technique

There are at least four subtle features of the integration technique that bear noting. Firstly, it is necessary to consider also texture components outside of H^0 since a spread of ε^0 can cause such components to have a presence in H^0 itself. In the present work this is most evident for the ideal *S* texture. The ideal *S* texture components, prepared taking this factor into account, is shown in Fig. 4. The influences of the (−27, 37, 59), (27, 37, 121), (56, 106, 53) and the (108, 58, 27) components, each of which spill over into H^0 in this case, are indicated. If these components are not taken into account then the mask will be slightly smaller than it should be. Secondly, it is recognised that if the different ideal orientations and their spreads are defined in a manner that allows them to overlap in Euler space, then $\sum_i V_i$ could be greater than unity. Thirdly, if the necessary volume is defined using an angular distance in the φ_2 and ϕ directions and a second angular distance in the φ_1 direction, then the resulting ideal texture component is actually cylindrical in shape, and it will enclose a 50% greater volume than the spherical ones shown here. (The ratio between the volumes enclosed by a cylinder of radius r and height $2r$, and a sphere of radius r is 1.5.)

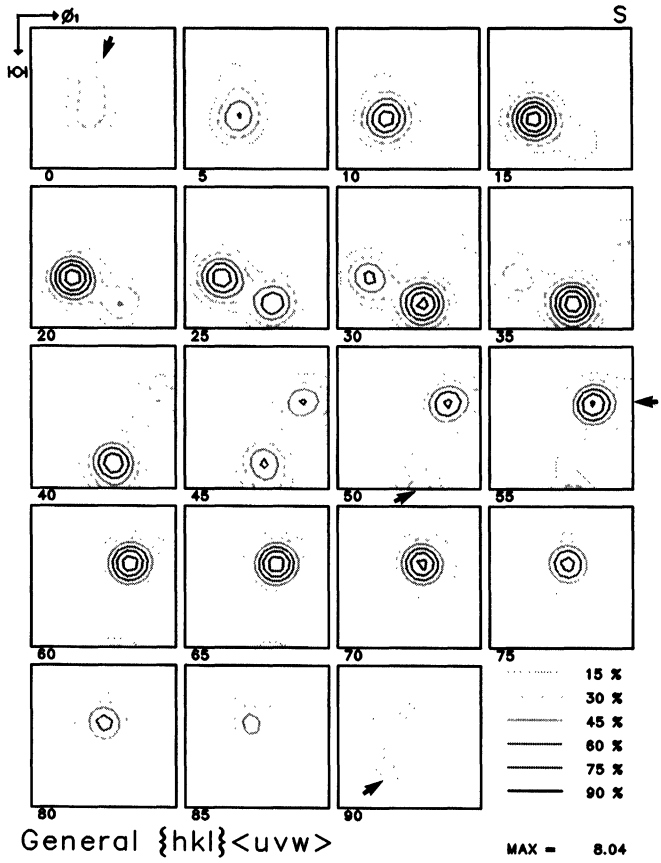

FIGURE 4 Ideal *S* texture, calculated as a Gaussian distribution with a spread of 15°.

However, unless the ODF was perfectly random, it does not follow that the *volume fraction* calculated with a cylindrical enclosure will actually be 1.5 times that calculated with a spherical one. Furthermore, whatever the shape of the enclosure, it could be constructed according to distances in Euler space (Eqs. (1) and (2)) or in Euclidean space (Eq. (11)), and this would affect the outcome of the calculation.

Finally, the magnitude of the volume fraction calculated depends quite critically on the 'spread' factor. This is because the volume of an enclosed region in space is proportional to the third power of the characteristic linear dimension. In a perfectly random texture the

texture volume fraction will therefore also be proportional to the cube of the spread. Of course, in many real textures the dependence between volume fraction and spread will be more complicated. For example, if the actual texture component is quite tightly focused, an increase in the spread parameter beyond a certain point will have little additional effect.

RESULTS

Orientation Distribution Functions

There was excellent qualitative agreement between the pole figures and ODFs obtained at Mintek and those reported for the same specimens by the industrial laboratory although, in general, the texture indices and maximum ODF values from Mintek were slightly larger. The comparative data for the specimens are listed in Table II, together with the calculated parameters for the two synthetic ODFs. It was reported by the industrial laboratory that their software did not correct for 'ghosts' (i.e. spurious negative ODF values). This may be the explanation for the slightly lower ODF values from the industrial laboratory. This would generally also tend to produce a lower texture index. The differences between the two sets of ODF are, however, not extreme and are compatible with the typical inter-laboratory scatter uncovered in round-robin testing by others, for example Vatne *et al.* (1996).

TABLE II Comparison of the ODF maxima and texture indices, as determined by two laboratories from the same samples

Sample	*ODF maximum (Mintek)*	*ODF maximum (industrial)*	*Index J (Mintek)*	*Index J (industrial)*
Random	1.00	—	1.0	—
Cube	33.0	—	11.1	—
DDH	13.27	13.44	3.2	3.8
HS19ED	6.57	7.00	2.2	3.0
HS19CE	7.72	6.63	2.6	2.6
DDI	10.43	9.01	1.8	1.7
1978	13.11	9.06	2.1	1.6
1982	8.81	5.94	1.6	1.4
1990	8.99	5.77	1.5	1.3
1996	8.83	5.62	1.7	1.4

Comparison of Volume Fractions in a Perfectly Random Texture

Since all orientations are equally represented in a perfectly random sample, it follows that such a sample must also contain a certain volume fraction of any ideal component, to an extent proportional to the number of times that symmetrically equivalent versions of that orientation occur (its 'multiplicity'). In addition, the volume enclosed by the ideal texture component depends rather strongly on the 'spread' assumed for that texture, since in general volume is proportional to the cube of a characteristic linear dimension. The Gaussian fitting method cannot be used in this case, since the ODF is everywhere equal to unity and no Gaussian can be fitted. Therefore only the integration method is applicable in this case, illustrating a deficiency of the Gaussian technique.

The effect of spread is shown in Fig. 5, for the particular cases of the volume fraction of the Goss texture in a perfectly random microstructure and in a hot-rolled aluminium sample (DDH). It can be seen that doubling the spread factor from 10° to 20° increases the volume fraction by a factor of nearly 8.

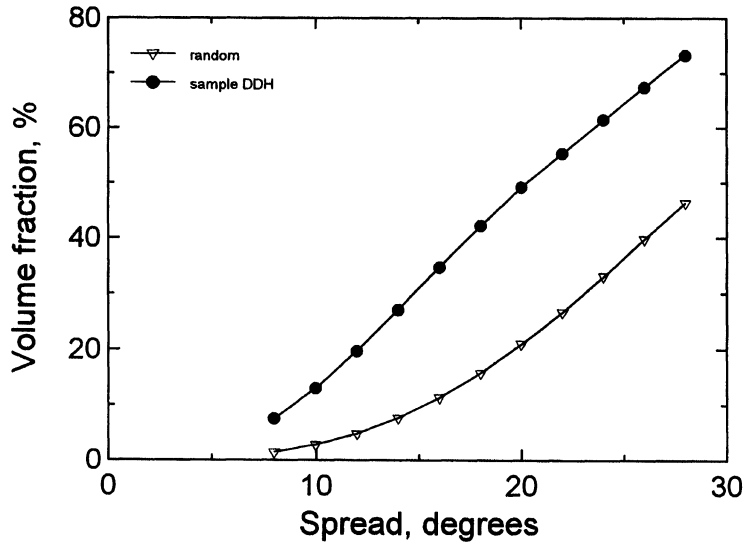

FIGURE 5 The effect of spread parameter on the volume fraction of S texture determined by integration using the present method.

TABLE III Comparison of the volume fractions given by various methods for the Goss texture in a perfectly random sample (all integrated with a 15° enclosure unless otherwise indicated)

Technique	*Method used*	*Volume fraction, %*
Euclidean sphere	integrated in Euler space	1.85
Euclidean cylinder	integrated in Euler space	2.91
Eulerian sphere	integrated in Euler space	2.25
	as above but 16.5° spread	3.04
	as above but 18.1° spread	4.0
Eulerian cylinder	integrated in Euler space	3.59
	as above but 15.5° spread	4.04
	as above but 16.5° spread	4.75
Industrial lab	integration of 'sphere'	3.5
Flower (1983)	integration of cylinder	3.4
Van Houtte (per comm)	integration of "sphere", 16.5° spread	4

The theoretical calculation of the volume fraction of the Goss or cube component has been reported by Flower (1983) and others (G. Marshall, personal communication) as being 3.4% for a 15° spread in a random sample. This would imply a 6.8% volume fraction for a brass or copper-type texture and 13.6% for the *S* texture. Similarly, for a 16.5° spread, Van Houtte (personal communication) has calculated the corresponding quantities to be 4%, 8% and 16%. As shown in Table III, use of a 15° Eulerian cylinder in the present software produces results that are compatible with those of Flower and the industrial laboratory. However, the volume fractions of Van Houtte are reached only with a sphere of radius 18.1° or a cylinder of spread 15.5°, indicating some small but significant difference in numerical integration procedures.

The volume fractions of a cube or Goss texture in a perfectly random sample, computed by different schemes are compared in Table III.

It is evident that the volume fractions of the perfectly random texture, computed with a cylindrical enclosure are, as predicted, about 1.5 times greater than those computed with a spherical enclosure.

Sample Volume Fractions Calculated using the Gaussian Fitting Technique

An example of the application of the Gaussian fitting technique to a sample in which the cube texture component is relatively well-expressed

is shown in Fig. 6. The Gaussian distribution of the cube-like texture components can be readily visualized in this case, and the relative RMS error of the regression technique was 14%. However, in cases where the texture component is not particularly well-developed, the meaning of a 'Gaussian' is diluted (Fig. 7). In this case the relative RMS error was 33%, and the values of the resulting ω_0 and S_0 parameters are of little physical significance. Therefore, the volume fraction calculated with Eq. (5) is of questionable use if the fit is poor or the data diffuse. Finally, in the case of a random or near-random texture the Gaussian tends to be very flat, wide and low in order to effect the best least-squares fit. In this case the tails of the Gaussian extend significantly outside of the 0–90° range of the H^0 subset of Euler space and a significant over-estimation of the volume fraction calculated by Eq. (5) results. This is because the Z symmetrically equivalent Gaussians now overlap through the various equivalent subsets of Euler space. Eq. (5) therefore applies only when the effective width of the Gaussian is well within 90°.

It should therefore be evident that the Gaussian fitting technique is suitable only for well-defined texture components. In the present work

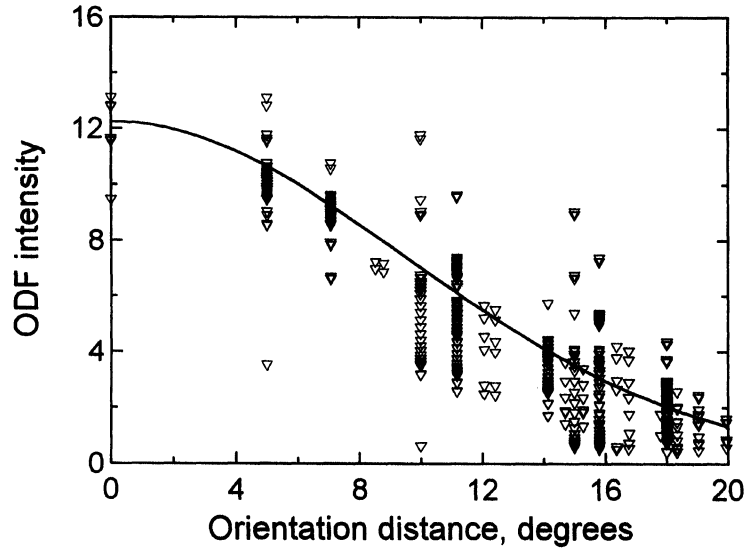

FIGURE 6 Gaussian profile of a well-developed cube texture component. The relative root-mean-square error of this fit was 14.3%.

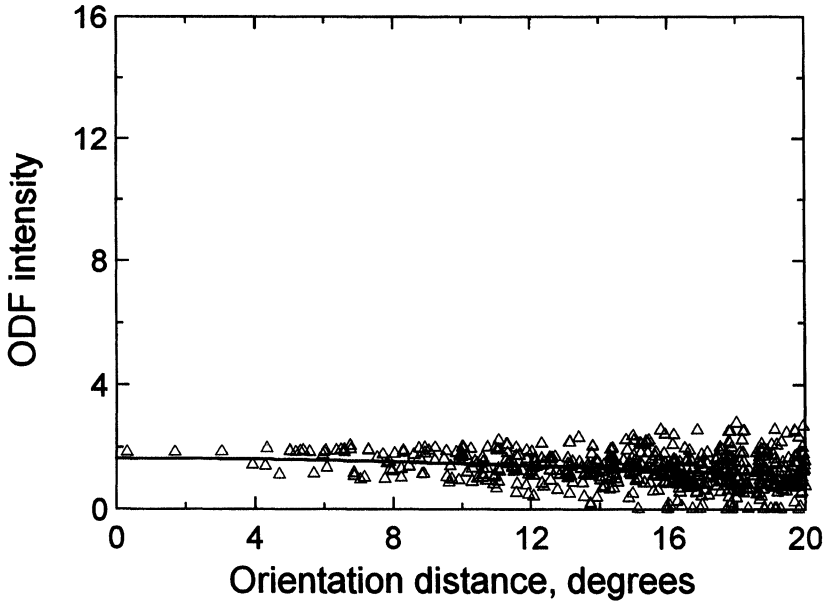

FIGURE 7 Attempt to fit a Gaussian profile through a poorly defined texture component ('copper' in an annealed specimen). The relative RMS error is 33%.

the cut-off spread on an ideal texture component is taken as 20°. Any ideal texture component with a greater spread is considered here to be too diffuse for further consideration. In general, in any case, the individual ODF values at orientation distances of greater than 20° are more likely to 'belong' to some other ideal texture component than the one involved in the calculation. (A possible exception could be a hypothetical sample that is made up only of very diffuse variations off a single ideal texture component.)

The results of applying this technique to the experimental samples are listed in Table IV. A volume fraction with less than 20% spread but with a relative RMS error greater than 25% is listed in Table IV in parentheses, indicating that it is somewhat problematic. It is evident that only 16 of the 50 possible calculations of volume fraction yielded usable volume fractions according to the criteria adopted. In general, less than half of the ODFs of the annealed samples could be satisfactorily explained as being the result of the ideal textures shown. However, in some of the ODFs the volume fractions listed totalled

TABLE IV Gaussian ideal components and their volume fractions. Volume fractions that are problematic shown in brackets. No volume fractions are shown for the distributions with spreads of greater than 20°

Sample	*Cube*		*Goss*		*Copper*		*Brass*		*S*	
	ω_0	%	ω_0	%	ω_0	%	ω_0	%	ω_0	%
Random	(171)	—	(101)	—	(91)	—	(88)	—	(87)	—
Cube	15.0	99.3	1.8	(2.6)	1.6	(1.4)	—	—	—	—
DDH	17.0	15.0	13.8	(5.2)	(21)	—	11.7	33.3	14.8	(72.9)
HS19CE	16.2	9.4	18.8	20.6	16.2	(27.2)	14.4	38.7	16.2	(75.3)
HS19ED	16.6	11.7	18.4	14.9	15.4	(24.5)	13.2	25.6	14.9	(56.8)
DD1	13.8	23.8	16.0	13.4	7.0	(1.7)	(28)	—	(21)	—
1978	13.4	26.5	16.6	(12.9)	(31)	—	(24)	—	(23)	—
1982	15.1	26.0	15.1	7.9	(29)	—	19.6	(22.2)	(26)	—
1990	13.7	19.2	20.1	(20.0)	5.0	(1.3)	(35)	—	(26)	—
1996	14.9	24.0	17.8	(13.4)	(60)	—	(27)	—	(31)	—

more than 100%. This was because the spread of two or more of the ideal components overlapped.

Sample Volume Fractions using the Eulerian Integration Techniques

The method in which a cylindrical enclosure in Euler space is integrated using the metric of Euler space was shown previously to be apparently the most compatible with the previous work of others in this field who have harnessed integration techniques. Accordingly, it has been isolated here for further consideration. The results of performing these integrations with an enclosure constructed using a 15° spread in both the $\phi-\varphi_2$ and the φ_1 sense are listed in Table V. In the case of most of the ideal textures considered here, only components actually falling within H^0 needed to be considered. However, the *S* ideal texture was slightly effected by components lying outside of H^0. The effect of this is evident in Table V, in which the column S^0 shows the volume fractions of the *S* texture computed from a mask constructed from only components lying within H^0, whereas the column marked S^* shows the volume fractions computed from a mask taking all sites inside or near to H^0 into account.

Sample Volume Fractions using the SPSE Technique

The results of using the single-point Euclidean technique coupled with the 'industrial' Euler positions shown in Table I are listed in Table VI.

TABLE V Volume fractions calculated using a cylindrical enclosure, constructed and integrated in Euler space

Sample	*Cube*	*Goss*	*Copper*	*Brass*	S^0	S^*
Random	3.8	3.6	7.2	7.0	14.3	14.6
Cube	54.7	0.3	2.1	1.9	0.3	0.3
DDH	6.2	3.1	13.8	23.7	39.4	40.1
HS19ED	5.2	6.1	13.4	16.9	32.8	33.4
HS19C	4.4	7.8	13.4	22.2	37.1	37.9
DD1	13.4	5.7	7.7	6.1	17.7	17.8
1978	14.9	5.3	9.6	8.6	22.5	22.7
1982	12.6	3.8	9.4	6.9	18.5	18.7
1990	10.9	5.8	8.0	6.4	17.1	17.3
1996	12.5	4.9	8.6	6.7	18.4	18.6

TABLE VI Determination of the volume fraction using the simplified single-point Euclidean technique

Sample	*Cube*	*Goss*	*Copper*	*Brass*	*S*
Random	4.0	3.8	7.3	7.3	13.9
Cube	29.2	0.1	1.2	2.5	3.9
DDH	7.1	4.0	11.9	28.7	37.7
HS19ED	6.9	7.0	14.8	20.1	34.7
HS19CE	5.6	10.3	14.8	27.0	40.2
DD1	15.2	5.4	5.8	4.6	13.0
1978	16.7	5.4	6.9	6.2	15.3
1982	14.4	3.9	7.1	6.3	13.4
1990	13.0	6.2	5.1	5.7	12.9
1996	11.8	5.5	7.3	5.7	14.1

Sample Volume Fractions Calculated by the Industrial Collaborator

The volume fractions reported by the industrial laboratory for the positions listed in Table I are shown in Table VII.

Scatter due to Specimen Preparation

Variations in sample preparation technique might also be expected to have some effect on the volume fractions. To gain an approximate indication of the magnitude of these effects, a sample of aluminium alloy 3004 was scanned three times to generate three ODFs. These ODFs are denoted WA1, WA2 and WA3 in Table VIII. The sample was then removed, electropolished a second time, and refitted in the same position as before, to yield ODF 'WA-POL'. Next the sample

TABLE VII Texture volume fractions reported by the industrial collaborator

Sample	*Cube*	*Goss*	*Copper*	*Brass*	*S*
Random	3.5	3.5	7	7	14
DDH	4.6	4.2	25.7	12.7	35.5
HS19ED	4.5	5.9	16.9	18.6	36.1
HS19CE	3.6	5.2	15.9	18.3	35.5
DD1	11.4	5.0	6.5	5.9	16.1
1978	11.2	4.7	7.8	6.9	17.4
1982	9.5	4.0	9.4	7.5	17.6
1990	8.9	4.8	7.7	6.8	16.2
1996	8.3	4.0	7.3	6.4	15.9

TABLE VIII Effect of sample preparation on the texture index and texture volume fractions

	WA1	WA2	WA3	WA-POL	WB	WC	$\bar{x}$	s
Texture index	4.20	4.21	4.24	3.51	3.64	5.17	4.16	0.59
Cube	19.63	19.53	19.55	19.59	19.73	19.94	19.66	0.15
Goss	4.16	4.29	4.11	4.67	4.59	3.35	4.20	0.47
Copper	2.23	2.21	2.14	2.07	2.00	2.87	2.25	0.31
Brass	3.68	3.64	3.84	4.75	4.27	2.87	3.84	0.64
S	7.58	7.17	7.14	7.82	7.68	7.67	7.51	0.21

was rotated by 180° and re-measured to give ODF 'WB', and finally, it was repositioned off-center in the stage and re-measured to give ODF 'WC'. The resulting volume fractions, computed by integration using a cylindrical enclosure of 15° radius and 30° height, are listed in Table VIII. It is evident that even re-measurement in the stage causes some variability in the ODFs calculated for a given specimen. However, re-preparation of the sample had quite a significant effect on the less important volume fractions, although relatively less effect on the major texture components. The results for samples HS19ED and HS19CE, shown in Table V, are also relevant. These refer to specimens cut from the edge and center respectively of a particular coil.

Texture volume fractions are, therefore, like any other physical parameter, subject to some scatter (about ±0.5 percentage points in this case), and if an accurate determination of their value is important than the appropriate statistical precautions should be taken. The variability shown in Table VIII may also be taken as a lower bound on the variation to be expected in intra-laboratory calculations of volume fractions using the present methods.

DISCUSSION

The integration technique described here is evidently suitable for simple ideal texture components based on specific values of {hkl}[uvw], and an integrated texture volume fraction based on Eulerian integration over a *spherical* ideal component may be a logical option for workers wishing to compare textures. The method described is not immediately suitable for fiber-type texture components, since these are sausage-shaped in Euler space. Nevertheless, as shown earlier, some of the previous workers have used a *cylindrical* enclosure. Therefore, in order to retain compatibility with such previous work, the set of Eulerian cylindrical results will be adopted here as the datum against which the others will be compared.

The texture volume fractions computed with Eulerian cylindrical integration, the SPSE and the industrial methods are compared in Fig. 8. It is evident that the three integration schemes produce answers that are very close in magnitude. In the case of the industrial method,

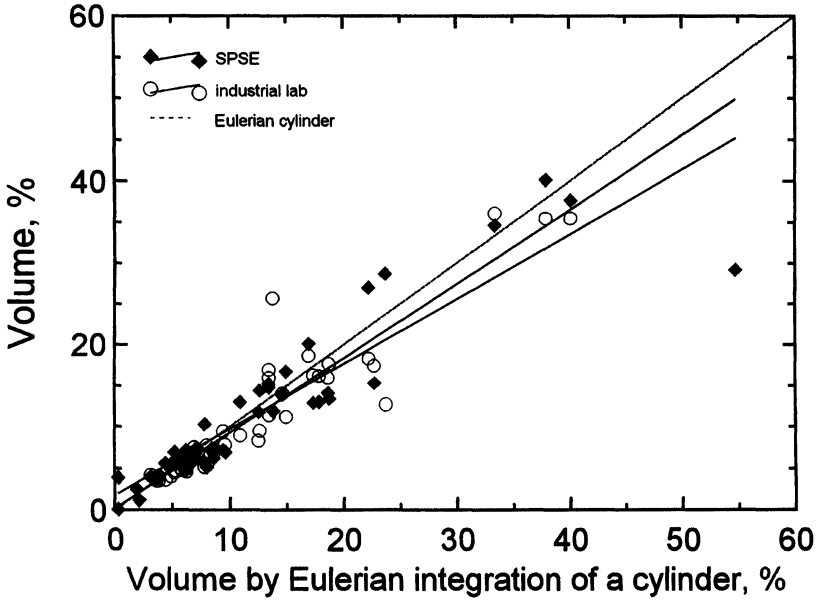

FIGURE 8 Comparison of the texture volume fractions computed by the three integration techniques.

the correspondence results because, although each laboratory was using different software and had re-measured the samples, the principles adopted were apparently similar. Similar reproducibility should be obtained between other laboratories using Eulerian integration of a cylindrical enclosure of radius 15° and height 30°. In the case of the SPSE method the excellent correspondence is, however, largely fortuitous, since that scheme operated in Euclidean space and had a spherical enclosure. Unless computation speed was for some reason very important, there seems to be no good reason to use the SPSE scheme, since it is based on some sweeping simplifying assumptions. The ranking of texture strengths produced by any of the integration schemes would be nearly the same, with some possible place-switching only for samples with components of very similar volume fraction.

As expected, Gaussian fitting followed by the application of Eq. (5) produced answers that were far larger than those produced by integration. This was due to the inclusion of the tails of the Gaussian, as mentioned previously. Nevertheless, if there was a genuine texture component with a rather large spread then it could be accurately ranked only by a Gaussian scheme or by an integration scheme with a correspondingly large spread. The significant difference between the Gaussian volume fraction of Eq. (5) and that produced by the various integration techniques can be narrowed by excluding the tails as follows.

A single shell of the volumetric integral over a Gaussian ideal texture is given by the area of a sphere (in Euler space) of radius r, multiplied by its thickness $\mathrm{d}r$, its average intensity from Eq. (3), the relevant crystallographic multiplicity, and the normalization factor of $1/(8\pi^2)$:

$$\mathrm{d}V_\mathrm{f} = 4\pi \cdot r^2 \cdot \mathrm{d}r \cdot S_0 \, \mathrm{e}^{-r^2/\omega_0^2} \cdot Z \cdot \frac{1}{8\pi^2}. \tag{12}$$

The total volume fraction up to an angular distance ω is given by

$$V_\mathrm{f} = \frac{Z \cdot S_0}{2\pi} \int_0^\omega r^2 \cdot \mathrm{e}^{-r^2/\omega_0^2} \mathrm{d}r. \tag{13}$$

This evaluates to

$$V_\mathrm{f} = \frac{S_0 \cdot Z \cdot \omega_0^2}{2\pi} \left[\frac{\omega_0 \cdot \sqrt{\pi}}{4} \mathrm{erf}\left(\frac{\omega}{\omega_0}\right) - \frac{\omega}{2} \exp\left(-\frac{\omega^2}{\omega_0^2}\right) \right]. \tag{14}$$

A further multiplication of Eq. (14) by a factor of 1.5 (the ratio between the volume of a cylinder over that of its enclosed sphere) should give approximately the same volume fraction as that produced by Eulerian integration over a cylinder of radius and half-height of 15°. The results are shown in Fig. 9, in which it can be seen that, although the results from the Eq. (14) multiplied by 1.5 are about 17% greater than those from the integration technique, there is an excellent correlation between the two. The small difference between the two methods is due to the factor of 1.5 being strictly correct only for a perfectly random ODF.

A simpler expression for volume fraction may be obtained by evaluating the integral in Eq. (13) up to $\omega = \omega_0$. Now we get

$$V_f = \frac{Z \cdot S_0 \cdot \omega_0^3}{2\pi} \cdot \left[\frac{\sqrt{\pi}}{4} \cdot \mathrm{erf}(1) - \frac{1}{2} e^{-1} \right]. \tag{15}$$

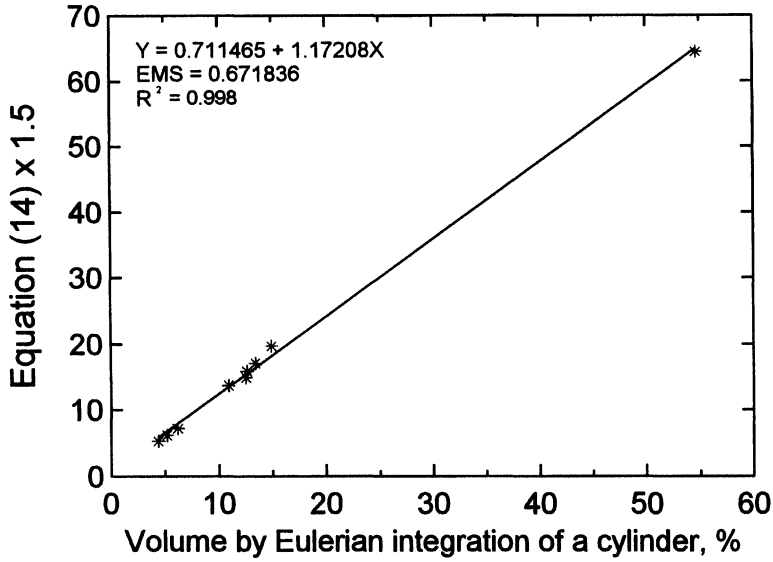

FIGURE 9 Correlation between cylindrical Eulerian volume fractions and those computed by Gaussian fitting up to a spread of 15° followed by a 50% correction to account for the increased volume of a cylinder.

which condenses to

$$V_f = 0.0302 \cdot Z \cdot S_0 \cdot \omega_0^3. \tag{16}$$

The Gaussian volume fractions computed for Eq. (16) are compared in Fig. 10 to those calculated by Eulerian integration over a *sphere* of the appropriate best-fitting radius ω_0. It is apparent that there is an excellent correlation between these two rather different methods of computing the volume fraction.

Finally, it should be possible to achieve Eq. (5) by integrating Eq. (15) up to ∞. However, the integral evaluates to

$$V_f = \frac{Z \cdot S_0 \cdot \omega_0^3}{8\sqrt{\pi}}, \tag{17}$$

which appears at first sight to be very different to Eq. (5). However, despite the difference in form, the application of Eq. (17) to the valid ideal components listed in Table IV yielded results that differed from

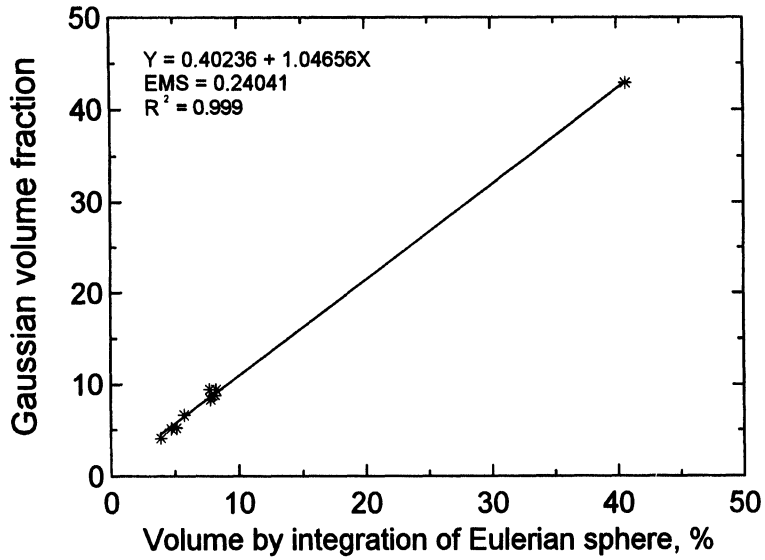

FIGURE 10 Correspondence between volume fraction derived by Gaussian fitting up to ω_0 with that derived by integration up to the same spread.

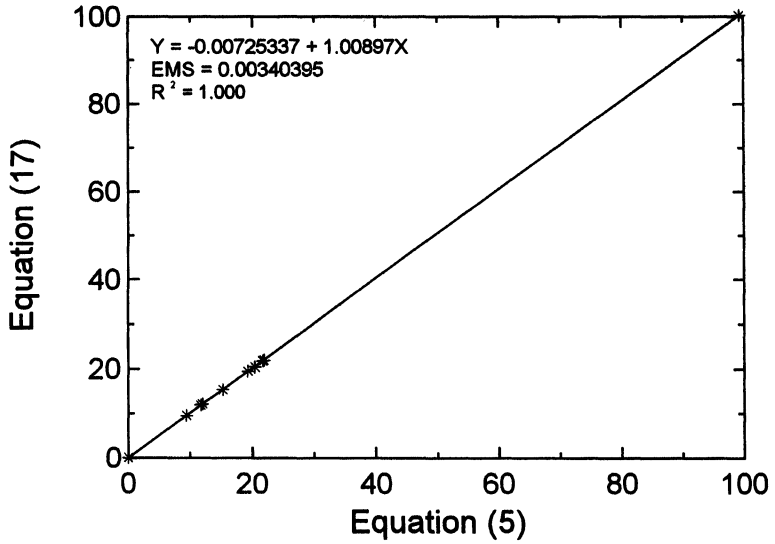

FIGURE 11 Correlation between the volume fractions of Eq. (5) with those of Eq. (17).

Eq. (5) by less than 1% of the respective values (Fig. 11). This is sufficiently close to make the two expressions functionally identical, with Eq. (17) being possibly preferred on account of its straightforward derivation and simpler form.

CONCLUSIONS

Reliable and reproducible texture volume fractions can be calculated from ODF data files provided that certain important factors are standardised. Although the most important of these is the angular spread considered to enclose the ideal component, the shape of the enclosing volume is also important. Provided that these factors are correctly accounted for, and provided that the ideal components really are distributed in an approximately Gaussian fashion, then the volumetric integration technique and the Gaussian fitting technique will give compatible answers. Furthermore, with respect to integration, calculation using a cylindrical enclosing volume will always give a larger volume fraction than calculation using a spherical enclosure.

Of the techniques available, calculation by integration is the most generally applicable, since methods based on the fitting of Gaussians will fail if the data around the component in question are too diffuse or irregular. The alternative technique, in which the ODF is computed from the C-coefficients of the harmonic series, requires that the method of spherical harmonic functions had been used, and is therefore not completely general in utility. Greatest compatibility with the work of others seems to require integration with a cylindrical enclosure; however, integration with a spherical enclosure may be more appropriate from a theoretical perspective. Usable texture volume fractions can be obtained by treating Euler space as a Euclidean space with coordinates φ_1, ϕ and φ_2, followed by integrating around components located as far as possible from the $\phi = 0$ plane. However, this seems to be an unnecessary simplification.

Acknowledgements

This paper is published by permission of Mintek and Hulett Aluminium, both of South Africa. The author wishes to especially thank Dr G. Marshall (Alcan International) and Mrs E. Jackson (Mintek) for performing the many measurements.

References

Bunge, H.J. (1982). *Texture Analysis in Materials Science*, Butterworths, London.

Bunge, H.J. (ed.) (1994). *Textures of Materials ICOTOM-10*, Materials Science Forum **157–162**, Trans Tech Publications, Aedermannsdorf, Switzerland.

Bunge, H.J. (1996). Physical versus mathematical aspects in texture analysis, *Textures and Microstructures* **25**, 71–108.

Flowers, J.W. (1983). Volume fractions of texture components of cubic materials, *Textures and Microstructures* **5**, 205–218.

Hansen, J., Pospiech, J. and Lücke, K. (1978). *Tables for Texture Analysis of Cubic Crystals*, Springer-Verlag, Berlin.

Ito, K., Musick, R. and Lücke, K. (1983). The influence of iron content and annealing temperature on the recrystallization textures of high-purity aluminium–iron alloys, *Acta Metall.* **31** (12), 2137–2149.

Jensen, D.J., Shi, H. and Bolingbroke, R.K (1994). Texture development in Al 3003 during hot strain compression, *Textures of Materials ICOTOM-10*, Materials Science Forum **157–162**, 745–752. Trans Tech Publications, Aederrnannsdorf, Switzerland.

Lücke, K., Pospiech, J., Jura, J. and Hirsch, J. (1986). On the presentation of orientation distribution functions by model functions. *Z. Metallkde.* **77**, 312–321.

Vatne, H.E., Oscarsson, A., Engler, O., Weiland, H., Reeves, A., Bate, P.S., Van Houtte, P., Zeng, X.H., Johnson, C., Funderberger, J.J., Zhou, Y., Fillit, R. and Bunge, H.J. Results from a round robin test on textures measured by X-ray diffraction, to be published in *Textures and Microstructures*.

Zuo, L., Muller, J. and Esling, C. (1994). A computer program for determining volume fractions of texture components in cubic materials, *Textures of Materials ICOTOM-10*, Materials Science Forum **157–162**, 493–499. Trans Tech Publications, Aedermannsdorf, Switzerland.